COMPENSATION OF TORQUE RIPPLE FOR BLDC MOTOR BASED ON FOPID CONTROLLER

K. Roja[1], M. Srikar[2], Dr. T. Anil Kumar[3]

[1]PG-Scholar, Department of EEE, Anurag University, Hyderabad, India.

[2]Assistant Professor, Department of EEE, Anurag University, Hyderabad, India.

[3]Head of Department, Department of EEE, Anurag University, Hyderabad, India.

kyasarlaroja@gmail.com[1], srikareee@cvsr.ac.in[2], hodeee@cvsr.ac.in[3]

Abstract:

The purpose of this project is to design and implement a controller for a Brushless DC Motor (BLDC) that use a Fractional Order Proportional-Integral-Derivative (PID) algorithm to mitigate torque ripple (FOPID). Because of commutation torque ripple, a six-step mode brushless dc motor (BLDCM) produces vibrational noise. In this piece, we'll go into what causes commutation torque ripple and what can be done about it, including topics like PWM-based predictive control and other methods (PWM-MPC). Predictive control may help get rid of torque ripple during commutation by adjusting the duty cycle based on a model of the system's behaviour. It's simpler to set up than other controllers since it doesn't need changing the motor driving circuit in any way. For anyone interested in experimenting with an alternative driving strategy beyond the typical square-wave, MATLAB/SIMULINK models of the suggested control system are available. We also look at the practicability of the plan. Simulation findings in this research suggest that the novel approach described here may significantly reduce torque ripple in comparison to traditional driving tactics.

Keywords: Model Predictive Control (MPC), Pulse Width Modulation (PWM), and Fractional Order Proportional Integral Derivative (FOPID) Controller for Brushless DC Motors (MPC).

DOI Number: 10.48047/NQ.2022.20.20.NQ109106 **NeuroQuantology2022;20(20): 1074-1083**

1. INTRODUCTION

As a result of its cheap production cost, high efficiency, and extended lifetime [1, 2], brushless dc motors (BLDCMs) are widely used in both consumer and industrial settings. However, torque ripple, especially that caused by periodic commutation, severely limits the BLDCM's performance. The mechanical noise and vibration that is produced by torque ripple renders it unfit for use in precision industries [4]. Reducing the BLDCM's torque ripple will boost its output. Several strategies have been studied as of late to reduce the commutation torque oscillations brought on by BLDCM. Kim et al. [5] devised a method for current-sensor-free output torque smoothing by deriving the commutation interval for the pulse width modulation from the terminal voltage (PWM). The torque ripple effects were reduced using a circuit in [6]. As a whole, it was a diode-clamped, multilayer inverter with three stages. In order to reduce the ripple in the commutation torque at low and high speeds, this method requires a high switching frequency. As described in [7-10], the authors' lightning-fast torque response and excellent steady-state performance were made possible through model predictive control. (MPC). There was no need for adjustment of the gain or the torque response. Modifying model variables within a precisely defined coordinate system may potentially lead to a state of control. Academics have looked at both the BLDCM and the hexagonal flux linkage locus [11]. The direct self-control method, which makes use of a switching point translation, is effective in delivering continuous torque performance while also increasing the control's range of motion. Using a tweaked Kaman filter and a sliding-mode observer, [12] devised a technique for sensor-free direct torque control. However, commutation failure might occur at higher motor speeds due to the short commutation gap. Guaranteeing reliable commutation and swiftly eliminating torque ripple, Shi and

eISSN 1303-5150

Li [13] devised a three-segment modulation strategy. To predict the commutation interval from the phase-current and dc voltage using the control methods provided in the aforementioned sources is a time-consuming and challenging endeavour. After investigating the root causes of torque ripple in a BLDCM, we provide a novel PWM-MPC approach for the speed closed-loop situation, where a predictive model is utilized to select the duty cycle of the power switches immediately before to commutation. From the collected data and analysis, we can deduce that the pulsation and ripple in the torque given to the output shaft while the motor is not commutating may be reduced.

2. PROPOSED SYSTEM

As seen in Fig. 1. A three-phase inverter, a motor, and a control module with programmed instructions make up the electrical components of the control system. The motor specifications used in the test, which reveal a two-pole pair BLDCM with a phase resistance of 0.75 ohm and a phase inductance of 1.048 mH. The simulation requires a continuous 24 V, which is provided by a dc power supply.An example of a FOPID-based PWM-system MPC's architecture is shown in this particular PWM-MPC employs Ha, Hob, and He coordinates for pinpoint positioning. Indicated the possibility that Hall signals may be used as a basis for calculating commutation moments.

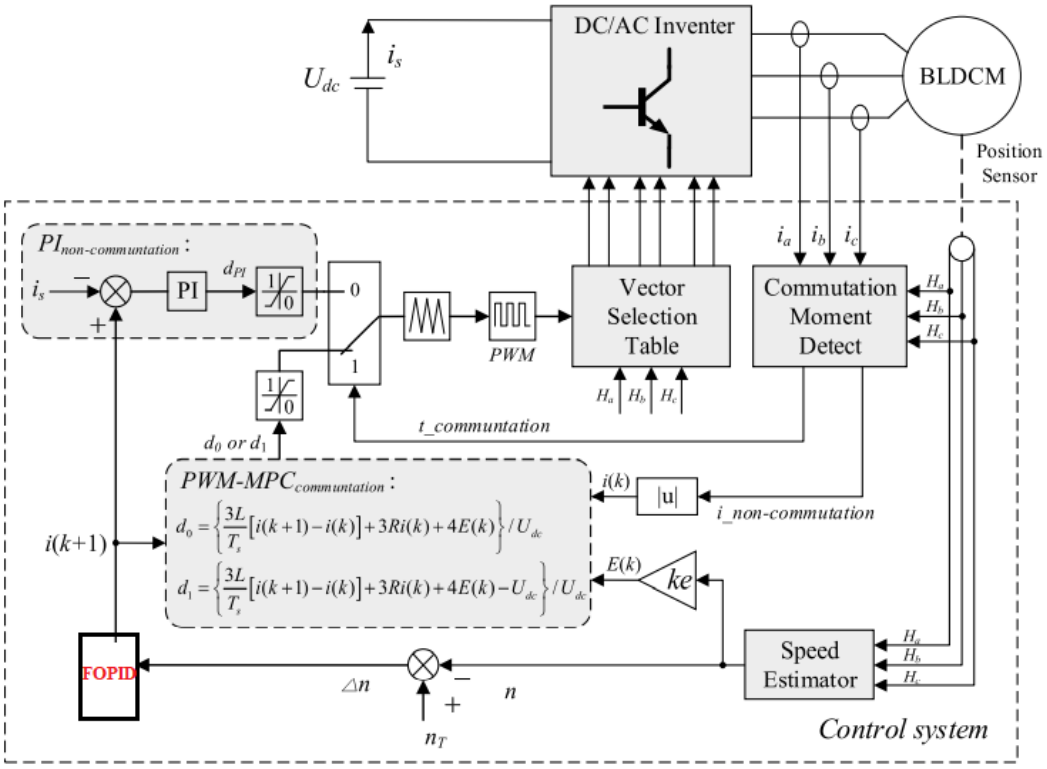

Fig.1: Proposed block diagram with PWM-MPC based on FOPID controller

eISSN 1303-5150

DETECTION OF COMMUTATION MOMENT

Commutation	Hall	Non-commutation current
AC→BC	H_b ↑	i_c
BC→BA	H_a ↓	i_b
BA→CA	H_c ↑	i_a
CA→CB	H_b ↓	i_c
CB→AB	H_a ↑	i_b
AB→AC	H_c ↓	i_a

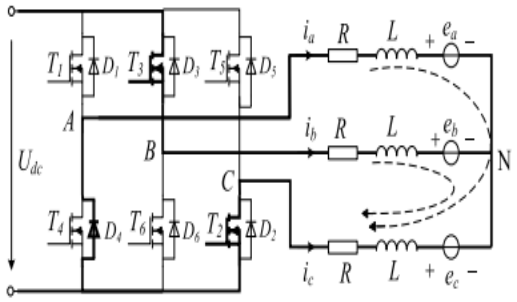

Fig.2: currents' direction of flow during commutation.

The torque ripple caused by cogging and other mechanical difficulties might be reduced by modifying the motor's design. In certain cases, the sensitivity of the armature may decrease as a result of the magnetic circuit layout. The commutation torque ripple is the most noticeable of the four forms of torque ripples that degrade a motor's performance throughout its six-stage operating mode [14]. If the rate of reduction of the outgoing phase current is not equal to the rate of increase of the incoming phase current, current pulsation may occur when the BLDCM is utilized for commutation. This is due to the inductance of the stator windings in conjunction with the voltage on the dc bus. Torque ripple, which may cause vibrations and noise, might reduce the BLDCM's performance [14] - [16]. The transition from alternating current (AC) to direct current (DC) will serve as an illustration.The commutation current flows through the circuit at 1 over the freewheeling diode D4. The voltage in the stator windings of a three-phase motor may be represented as

$$\begin{bmatrix} u_A \\ u_B \\ u_C \end{bmatrix} = \begin{bmatrix} R & 0 & 0 \\ 0 & R & 0 \\ 0 & 0 & R \end{bmatrix} \begin{bmatrix} i_a \\ i_b \\ i_c \end{bmatrix} + \begin{bmatrix} L & 0 & 0 \\ 0 & L & 0 \\ 0 & 0 & L \end{bmatrix} \frac{d}{dt} \begin{bmatrix} i_a \\ i_b \\ i_c \end{bmatrix} + \begin{bmatrix} e_a \\ e_b \\ e_c \end{bmatrix} + \begin{bmatrix} u_N \\ u_N \\ u_N \end{bmatrix} = \begin{bmatrix} 0 \\ U_{\text{dc}} \\ 0 \end{bmatrix} \quad (1)$$

$$i_a + i_b + i_c = 0. \quad (2)$$

If the back EMF is equal to E and stays constant throughout the commutation, then uN can be represented as

$$u_N = \frac{U_{\text{dc}} - E}{3}. \quad (3)$$

eISSN 1303-5150

To conclude, if the phase resistance is zero, we get condition (2) and condition (3). (1). Three-stage slope rates may be stated as (4). In Fig. Figure 1 indicates that there are three unique kinds of commutation-induced current ripples dependent on the slope rates of the currents. 2. Please refer to Fig. It reaches saturation in t1, the same time period as the phase current if.

$$\begin{cases} \dfrac{di_a}{dt} = \dfrac{-U_{dc} - 2E}{3L} \\ \dfrac{di_b}{dt} = \dfrac{2U_{dc} - 2E}{3L} \\ \dfrac{di_c}{dt} = \dfrac{-U_{dc} + 4E}{3L}. \end{cases} \tag{4}$$

$$\begin{cases} \dfrac{di_a}{dt} + \dfrac{di_b}{dt} > 0 \\ \dfrac{di_c}{dt} < 0. \end{cases} \tag{5}$$

$$\begin{cases} \dfrac{di_a}{dt} + \dfrac{di_b}{dt} < 0 \\ \dfrac{di_c}{dt} > 0. \end{cases} \tag{6}$$

We have shown that in each of these scenarios, changes in the non-commutation current will result in different levels of output torque. Varying the time spent in the initial departure phase (t0) or the succeeding, continuing phase (t1) may reduce the torque ripple and keep the ice slope rate constant.

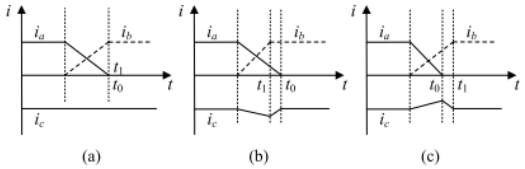

Fig. 3: Characteristics right now throughout the commute. There is a non-commutation current. (a) constant, (b) convex, and (c) concave.

PWM-MPC Strategy to Minimize the Torque Ripple

rate at which the outgoing phase current is falling is less than the rate at which the incoming phase current is growing. During commutation, a higher bus voltage is required to speed up the slots for the phase current leaving the power plant (4). But a complicated auxiliary hardware circuit is required. A slower increase in phase current may be achieved by adjusting the switch's duty cycle. Since no extra hardware circuits are required, the approach can be quickly implemented. Consequently, the commutation ripple may be reduced by altering the rising time of the incoming phase current. Consider how commutation alters the flow of electricity by changing it from alternating current (AC) to direct current (DC) (DC). The letters DB denote the duty cycle used while phasing in B. Power supplied in three stages, or "phases," may be written as

eISSN 1303-5150

$$\begin{cases} u_A = Ri_a + L\dfrac{di_a}{dt} + e_a + u_N = 0 \\ u_B = Ri_b + L\dfrac{di_b}{dt} + e_b + u_N = D_B \times U_{\mathrm{dc}} \\ u_C = Ri_c + L\dfrac{di_c}{dt} + e_c + u_N = 0. \end{cases} \quad (7)$$

$$u_{BC} = -3L\frac{di_c}{dt} - 3Ri_c + 4E = D_B \times U_{\mathrm{dc}}. \quad (8)$$

The duty cycle of the switch tube in the incoming phase is defined as d0. Consequently, d0 is content with

$$d_0 = \left\{\frac{3L}{T_s}[i(k+1) - i(k)] + 3Ri(k) + 4E(k)\right\} \Big/ U_{\mathrm{dc}} \quad (9)$$

We utilize the forward Euler method, assuming a time step of Ts. Assuming the non-commutation phase current is held constant at a value equal to the projected current, things will be much simpler. I (k + 1) = I (k), where I (k) is the provided current, since the output of the speed close loop at time k is equal to the supplied current. At Duck 4E, the properties of the current and torque change from those seen when Duck > 4E. To get higher gains during commutation, as shown in, a hardware circuit is necessary (4).

$$\begin{cases} u_A = Ri_a + L\dfrac{di_a}{dt} + e_a + u_N = D_A \times U_{\mathrm{dc}} \\ u_B = Ri_b + L\dfrac{di_b}{dt} + e_b + u_N = U_{\mathrm{dc}} \\ u_C = Ri_c + L\dfrac{di_c}{dt} + e_c + u_N = 0. \end{cases} \quad (10)$$

DA might be created by combining (2) and (10), as in

$$u_{AC} = -3L\frac{di_c}{dt} - 3Ri_c + 4E - U_{\mathrm{dc}} = D_A \times U_{\mathrm{dc}} \quad (11)$$

Define d1 similarly as the function of the departing phase. d1 might be provided as

$$d_1 = \left\{\frac{3L}{T_s}[i(k+1) - i(k)] + 3Ri(k) + 4E(k) - U_{\mathrm{dc}}\right\} \Big/ U_{\mathrm{dc}} \quad (12)$$

By using an advanced Euler method, which involves working backwards. The MPC keeps the current constant throughout the off-commutation period by controlling the duty cycle of the commutation phase.

eISSN 1303-5150

3. PROPOSED FOPID CONTROLLER

In industrial control systems, PID controllers are the de facto standard feedback control loop technique. Any time a consistency process variable deviates from the desired set point, the PID controller formulates and executes a plan of action to bring it back to where it should be.

The transfer function of a PID controller with integer orders looks like this:

$$G_c(S) = K_p + K_s s^{-1} + K_d s \tag{13}$$

Integral (Kid) and derivative (Kid) time constants are used in developing the PID controller. These are the pillars upon which the PID control approach rests. The Integral, which depends on the Relative gain, the sum of recent errors, and the rate of error change, regulates the error reaction. By combining these three actions, a valve or heater may be utilized to control the process. Figure 4 depicts a closed-loop system using a PID controller.

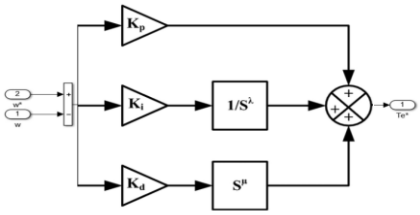

Fig. 4: FOPID controller

4. SIMULATION RESULTS

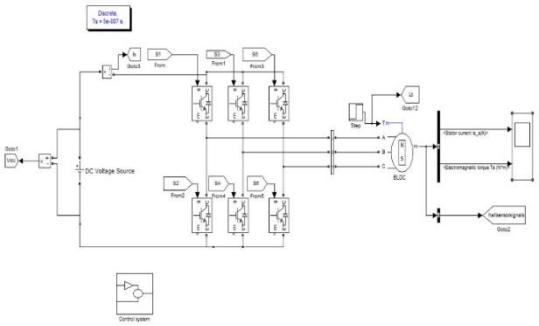

Fig. 5: MATLAB/SIMULINK circuit diagram of the proposed system

A) RESULTS WITH PI CONTROLLER

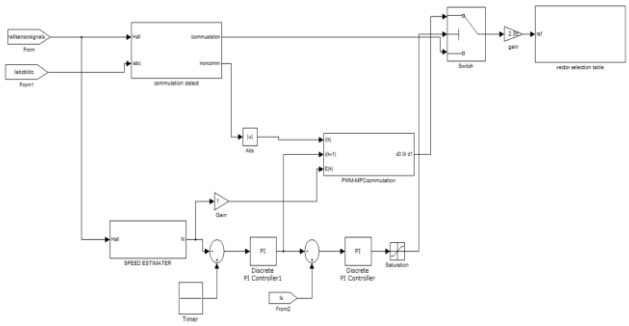

Fig.6: Control system

eISSN 1303-5150

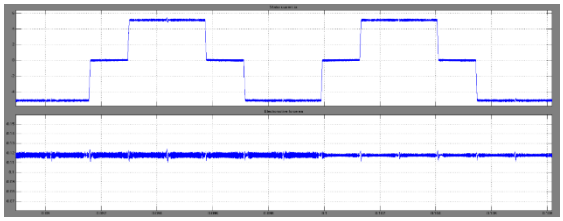

(a) Current and Torque of the stator

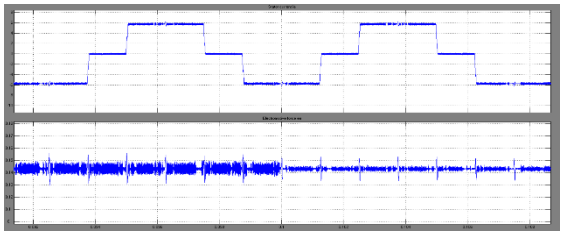

(b) Current and Torque of the stator

Fig.7: Simulation waveforms of the BLDCM. Simulation results at a speed of (a) 500 and (b) 1500 r/min

B) RESULTS WITH FOPID CONTROLLER

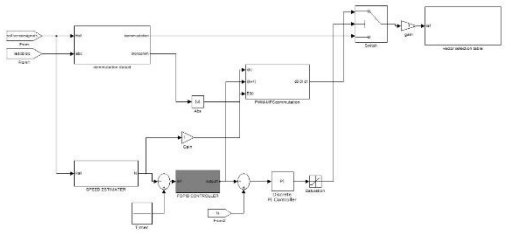

Fig 8. Control system with FOPID controller

Fig8. Using a constant load of 0.1 Nm, BLDCM simulations were ran at 500 and 1500 rpm, the results of which are shown in Fig. 9. After 0.1 s, a PWM-MPC using a FOPID controller takes over from the PI closed-loop control mechanism. Torque is maximized when phase currents are convex, as they are during commutation. A total of less than 0.1 second is being discussed. By varying the phase current's duty cycle, the required commutation voltage may be generated in < 0.1 s. The magnitude and frequency of current and torque fluctuations are noticeably reduced. In Fig. Figure 9 shows that the incoming phase current increases quicker than the departing phase current drops at 1500 rpm (b). As a result, the phase currents have a concave form just before commutation (at 0.1 s). A drop in the duty ratio of the phase current will increase the electromagnetic torque shortly after 0.1 s. As a result, torque variations are reduced. In my head, I've set this number at this value. Figure 10 shows the results of a simulation testing the BLDCM's performance at 250 and 1000 rpm while under a continuous 0.1 Nm load.

eISSN 1303-5150

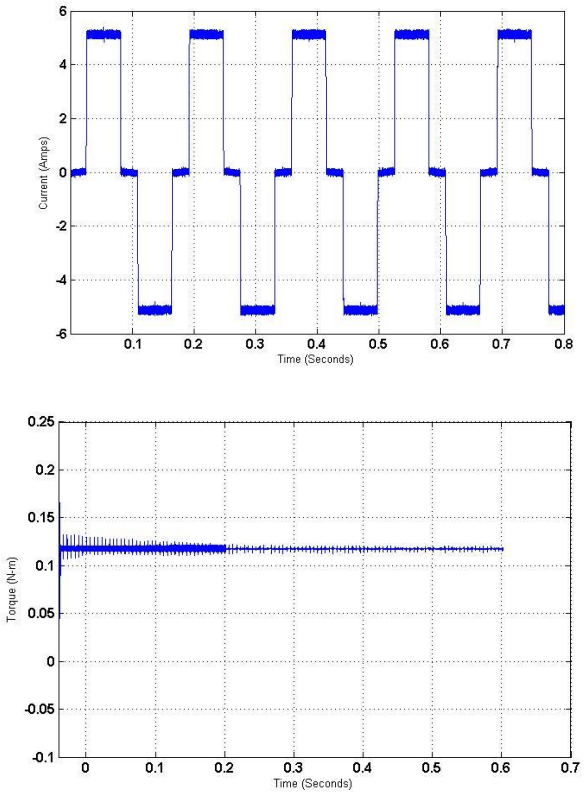

(a) Current and Torque of the stator

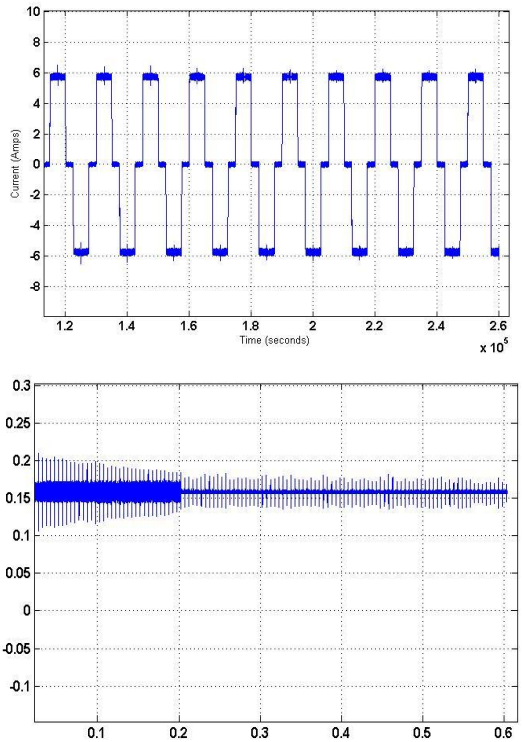

(b) Current and Torque of the stator

Fig.9: Simulation waveforms of the BLDCM. Simulation results at a speed of (a) 500 and (b) 1500 r/min

eISSN 1303-5150

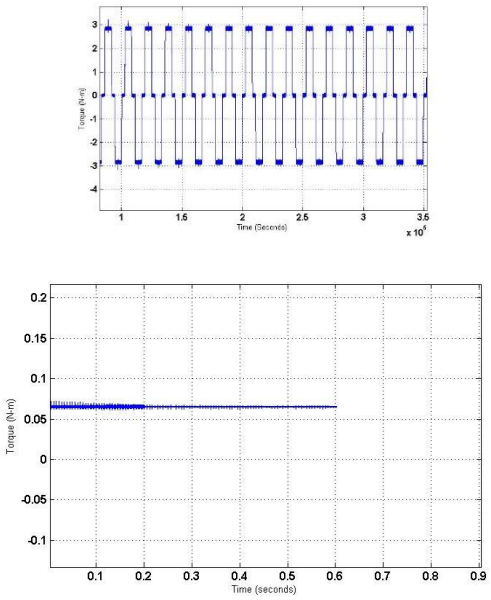

(a) Current and Torque of the stator

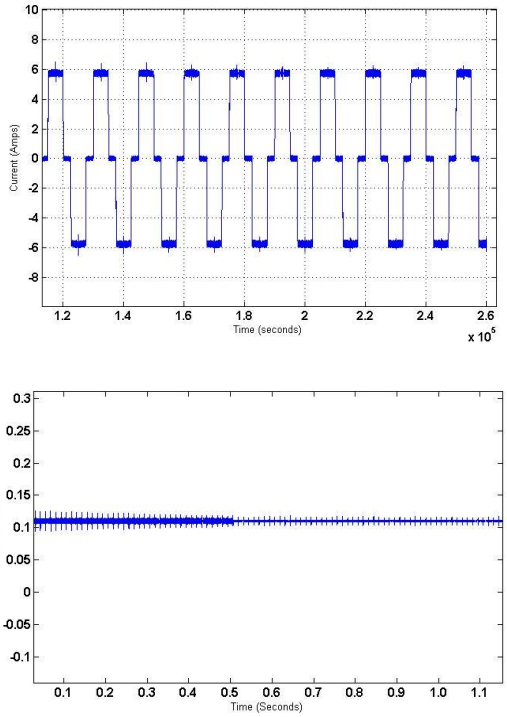

(b) Current and Torque of the stator

Fig.10: Simulation waveforms of the BLDCM. Simulation results at a speed of (a) 250 and (b) 1000 r/min

5. CONCLUSION

This study introduces a novel PWM-MPC based on a FOPID control strategy for the BLDCM. The effectiveness of the proposed FOPIDC control mechanism was confirmed by simulations. The results show that PWM-MPC based on the FOPID approach might possibly reduce current ripple and torque ripple at low and high speeds without altering the circuit design.

eISSN 1303-5150

REFERENCES

[1] K. Xia, J. Lu, C. Bi, Y. Tan, and B. Dong, "Dynamic commutation torque-ripple reduction for brushless DC motor based on quasi-Z-source net," IET Electra. Power Appl., vol. 10, pp. 819–826, Nov. 2016.

[2] G.-J. Su and J. W. Makeover, "Low-cost sensor less control of brushless DC motors with improved speed range," IEEE Trans. Power Electron., vol. 19, no. 2, pp. 296–302, Mar. 2004.

[3] Y.-C. Son, K. Y. Jang, and B.-S. Suh, "Integrated MOSFET inverter module for low-power drive system," IEEE Trans. Ind. Appl., vol. 44, no. 3, pp. 878–886, May/Jun. 2008.

[4] K. Xia, Z. Li, J. Lu, B. Dong, and C. Bi, "Acoustic noise of brushless DC motors induced by electromagnetic torque ripple," J. Power Electron., vol. 17, no. 4, pp. 963–971, 2018.

[5] D.-K. Kim, K.-W. Lee, and B.-I. Kwon, "Commutation torque ripple reduction in a position sensor less brushless DC motor drive," IEEE Trans. Power Electron., vol. 21, no. 6, pp. 1762–1768, Nov. 2006.

[6] V. Viswanathan and J. Seenithangom, "Commutation torque ripple reduction in the BLDC motor using modified SEPIC and three-level NPC inverter," IEEE Trans. Power Electron., vol. 33, no. 1, pp. 535–546, Jan. 2018.

[7] A. G. Castro et al., "Finite control-set predictive power control of BLDC drive for torque ripple reduction," IEEE Latin Amer. Trans., vol. 16, no. 4, pp. 1128–1135, Apr. 2018.

[8] J. Rodriguez et al., "Predictive control of three-phase inverter," Electron. Lett., vol. 40, no. 9, pp. 561–563, Apr. 2004.

[9] P. Liana, R. Aguilera, and D. E. Quevedo, "Model predictive control of an asymmetric flying capacitor converter," IEEE Trans. Ind. Electron., vol. 56, no. 6, pp. 1839–1846, Jun. 2009.

[10] S. Müller, U. Ammann, and S. Rees, "New time-discrete modulation scheme for matrix converters," IEEE Trans. Ind. Electron., vol. 52, no. 6, pp. 1607–1615, Dec. 2005.

[11] C. Xia, H. Chen, X. Li, and T. Shi, "Direct self-control strategy for brushless DC motor with reduced torque ripple," IET J., vol. 12, no. 3, pp. 398–404, 2018.

[12] Y. Liu, Z. Q. Zhu, and D. Howe, "Instantaneous torque estimation in sensor lessdirect-torque-controlled brushless DC motors," IEEE Trans. Ind. Appl., vol. 42, no. 5, pp. 1275–1283, Sep./Oct. 2006.

[13] J. Shi and T.-C. Li, "New method to eliminate commutation torque ripple of brushless DC motor with minimum commutation time," IEEE Trans. Ind. Electron., vol. 60, no. 6, pp. 2139–2146, Jun. 2013.

[14] C. Bi, Q. Jiang, S. Lin, T. S. Low, and A. A. Mamun, "Reduction of acoustic noise in FDB spindle motors by using drive technology," IEEE Trans. Man., vol. 39, no. 2, pp. 800–805, Mar. 2003.

[15] F. Rodriguez and A. Meade, "A novel digital control technique for brushless DC motor drives," IEEE Trans. Ind. Electron., vol. 54, no. 5, pp. 2365–2373, Oct. 2007.

[16] V. Viswanathan and S. Jeevananthan, "Approach for torque ripple reduction for brushless DC motor based on three-level neutral-pointclamped inverter with DC–DC converter," IET Power Electron., vol. 8, no. 1, pp. 47–55, Jan. 2015.

[17] J. Fang, H. Li, and B. Han, "Torque ripple reduction in BLDC torque motor with nonideal back EMF," IEEE Trans. Power Electron., vol. 27, no. 11, pp. 4630–4637, Nov. 2012

eISSN 1303-5150